Propulsion and Power Research 2020;9(3):216−224

http://ppr.buaa.edu.cn/

Propulsion and Power Research

www.sciencedirect.com

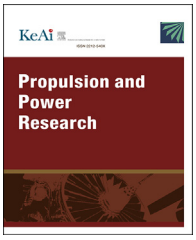

ORIGINAL ARTICLE

Catalytic effect of platinum and silver in a hydrogen peroxide monopropellant ceramic microthruster

Zahra Khaji[a,b,*], Lena Klintberg[b], Kristoffer Palmer[c], Greger Thornell[a,b]

[a] *Ångström Space Technology Centre, Department of Engineering Sciences, Uppsala University, Box 35, Uppsala, 75103, Sweden*
[b] *Division of Microsystems Technology, Department of Engineering Sciences, Uppsala University, Box 35, Uppsala, 75103, Sweden*
[c] *Nanospace AB, Ulls Väg 29A, Uppsala, 75651, Sweden*

Received 25 November 2019; accepted 28 August 2020
Available online 15 September 2020

KEYWORDS

Monopropellant microthruster;
HTCC;
Catalytic bed;
Platinum;
Silver;
Hydrogen peroxide;
Electroplating

Abstract Ceramic microthrusters with an embedded Pt resistive heater, two temperature sensors, and a Pt or Ag catalytic bed were made of high-temperature co-fired alumina ceramics. To increase the surface area by a factor of 1.21, and so the catalytic effect, the Pt catalytic bed was made porous by mixing the Pt paste with 15−20vol.% graphite sacrificial paste before screen printing it. Ag was in-situ electroplated on the porous Pt surface after sintering. Decomposition of 50wt.% hydrogen peroxide as a monopropellant was studied both qualitatively and quantitatively by changing the catalyst (between Ag and Pt), flow rate (15−55 μl/min), and operating temperature (115−300 °C). A reference device without catalyst exhibited an unstable behavior as a result of no, or very little, decomposition, whereas the Ag catalyst was more stable, and the Pt one even more stable. Also, Pt was found to be slightly more effective. Quantitatively, there were small differences between Pt and Ag in the power needed to maintain the temperature. The

*Corresponding author.
E-mail address: zahra.khaji@angstrom.uu.se (Zahra Khaji).
Peer review under responsibility of Beihang University.

ELSEVIER | Production and Hosting by Elsevier on behalf of KeAi

https://doi.org/10.1016/j.jppr.2020.08.003

inventive methods to make the Pt bed porous as well as in-situ electroplating Ag were successfully demonstrated.

1. Introduction

There is usually both a primary and a secondary propulsion system on a satellite [1]. The primary one is used to change the orbit or to perform an end-of-life maneuver, and requires thrusters that can deliver high thrusts, or high specific impulses. The secondary propulsion system, on the other hand, is used for precise attitude and positioning control. For maneuvers used to compensate for disturbances, such as solar radiation pressures, both a certain thrust range and a small enough minimum impulse are essential [2]. Sometimes, large, low-thrust devices can be used, but for very small satellites (<10 kg) operated at thrust levels in the range of micro-to millinewton, miniature thrusters are required. Microelectromechanical systems (MEMS) technology, also known as Microsystems Technology (MST), offers extreme miniaturization. Using manufacturing techniques such as lithography, etching, deposition, etc., MST also provides a high level of integration of components. Hence, it is a promising option for the secondary propulsion system of small satellites.

In liquid monopropellant microthrusters, the propellant is decomposed in presence of a catalyst. Compared with a gaseous propellant, a liquid can be stored more compactly and with less risk of leakage. Furthermore, unlike solid propellant thrusters, the liquid propellant ones can readily be stopped and restarted [3]. MEMS thrusters of this type can deliver thrusts in the range of 10−200 mN [3], making them a suitable alternative for attitude control.

Of greatest importance to consider when designing a monopropellant microthruster, is the choice of propellant, which will have direct influence on the choice of catalyst and structural materials. The three most commonly used monopropellants are hydrogen peroxide, hydroxylammonium nitrate (HAN), and hydrazine [4]. Of these, hydrogen peroxide is the least expensive and least toxic one. Moreover, its decomposition products are water and oxygen, which, of course, are environmentally friendly. High-concentration hydrogen peroxide has a long history of application in aerospace propulsion and power systems. Dating back to the 1930s, there are numerous applications of hydrogen peroxide systems for both manned and unmanned missions [5]. However, the use has decreased since the 1960s, as hydrogen peroxide has been substituted by propellants such as hydrazine with higher specific impulse and long-term stability. Recently, hydrogen peroxide has been receiving a renewed interest, since handling highly toxic propellants is becoming increasingly expensive [5], and some of them may even be banned in the near future [6].

Almost all types of catalyst, i.e., heterogeneous, homogeneous, and enzyme-based ones, can be used for decomposition of H_2O_2 [7]. Silver is a widely used catalyst for several reactions [8] and is the most common and oldest catalyst for hydrogen peroxide in space industry. However, there are concerns regarding its long-term stability, since so called poisoning of the catalyst occurs as a result of chemical reactions with the additives in the propellant, and this reduces the catalytic effect. Therefore, other catalyst alternatives such as manganese dioxide (MnO_2) and other precious metals such as platinum-group metals are being investigated [9].

There are other parameters that play a significant role in the catalytic behavior. For instance, metal catalysts with different sizes and structures show different catalytic behaviors [10]. Also, to increase the performance of catalyst-enhanced reactions, the relative surface area of the catalyst material can be increased. Here, miniaturization works in favor, since the ratio of surface area to volume (and mass) increases. In addition, the surface can be structured or textured to increase its effective area. Therefore the choice of a proper catalyst for a specific microthruster has to be investigated thoroughly.

As shown in [11], the wall temperature of hydrogen peroxide propellant microthrusters can be 630 °C or higher. Unfortunately, this is above the long-term temperature tolerance of silicon, the perhaps most established material for microcomponents [12]. Therefore alternative materials should be considered. Furthermore, since many liquid propellants are corrosive, a high chemical resistance is important both for the nozzle and for its interconnects.

Except maybe for the connection issue, ceramics offer a promising option. Although co-fired ceramic technology has been used for packaging for a long time in the electronics industry, it is quite recently that it has become a means to manufacture microcomponents. The technology is based on machining soft, unsintered ceramic tapes, adding conductors by screen printing, and, after lamination, sintering the ceramic and conductive parts together.

In this work, a study of the catalytic effect of Pt and Ag when 50wt.% hydrogen peroxide is used as a propellant is conducted. For this purpose, microthrusters based on the design in [13] are manufactured in alumina. These thrusters have a heater, two temperature sensors and a porous catalytic bed, all integrated in a single chip, and are evaluated

with respect to behavior versus propellant flow rate and temperature. For comparison, a thruster without a catalytic bed is used. Furthermore, a probe fixture is introduced to overcome the electrical and fluidic interface challenges faced in the literature. To circumvent the limitations with catalysts compatible with sintering of the alumina, post-sintering, inter-cavity electroplating is attempted. To facilitate texturing of the catalyst to increase its effective area, it is made porous by including sacrificial carbon. Both these steps are pioneering.

It should be emphasized that this is an exploratory, innovative, and mostly qualitative study, striving to add to the very limited research presented in the field of monopropellant microthrusters in general, and ceramic ones in particular.

2. Background

There are several studies on the catalytic behavior of different materials on the decomposition of hydrogen peroxide. Ventura et al. [14] have evaluated a large group of catalysts, and concluded that silver is the most efficient one for 90wt.% H_2O_2. In [15], the authors found silver to be more efficient than platinum for 30wt.% hydrogen peroxide. In agreement with the results of these studies, Pirault-Roy et al. [16] reported silver to be the most active catalyst, followed by manganese oxides and platinum. However, in a study conducted by Rusek that is cited in [17,18], it was shown that platinum on alumina, followed by manganese oxides, was much more active with rocket grade hydrogen peroxide compared to silver and silver oxide. Another study on catalysts for 30wt.% H_2O_2 [19], suggested that Pt was the most promising candidate, followed by ruthenium oxide, palladium, and manganese oxides, all of which were deposited on alumina. Silver was not included in this last study, though. These discrepancies show that further research is required, especially when targeting micropropulsion.

When used with catalysts such as Ag or MnO_2, the catalytic onset temperature of hydrogen peroxide is reported to be around room temperature (25−30 °C) [20]. Platinum has been shown to be active even slightly below this [13].

Regarding texturing the surface of the catalyst, Takahashi et al. [21], for instance, have investigated various methods, including liquid phase deposition of platinum nanoparticles on silicon having pores with a diameter of 1−2 μm. For the microthruster made in [22], a 1 μm thick silver layer was vapor deposited on microstructured silicon pillars, and in [23], a catalyst of chemically synthesized MnO_2 nanowire was dispensed inside a micromachined thruster chamber with a burette.

Although a number of cold gas, vaporizing liquid, and solid propellant [24−28] microthrusters have been made with low-temperature and high-temperature co-fired ceramics (LTCC and HTCC) technology, only a few examples of using ceramics to make liquid propellant thrusters have yet been published.

Wu et al. [29] have characterized a HAN-based monopropellant LTTC microthruster using Ag electrodes as both ignitor and catalyst, and achieved a thrust of ~200 mN. Markandan et al. have investigated a HAN-based propellant with thrusters made of alumina-toughened zirconia (ATZ) with yttria-stabilised zirconia-graphene (YSZ-Gr) electrodes [30]. Using electrolytic decomposition without any catalyst, a maximum thrust of about 180 mN was recorded. This was, however, only 50% of the thrust expected. Although, not realizing any component, Plumlee et al. [31] have shown that LTCC, and hence other ceramics exhibiting a low thermal conductivity, are suitable for hydrogen peroxide microthrusters. Using gel casting in PDMS soft molds, a zirconia microthruster has been manufactured, but not tested with any propellant [32]. A monopropellant microthruster made of alumina HTCC, with an integrated resistive heater and two resistive temperature sensors, and employing a platinum catalytic bed, was presented in [13]. This work was focused on how the dry operation temperature tolerance was affected by the designs, but the device was also characterized using 31wt.% hydrogen peroxide as a propellant.

In other works, the tube that feeds the microthrusters with propellant has been glued to the inlet with epoxy [22,25,32,33], or a ceramic cement [34]. With increasing temperature, the propellant becomes increasingly corrosive against adhesives. In addition, thermal mismatch can cause failure. Thus, a more robust connection is necessary in order to increase the service temperature of the thruster. In [31], a test stand, where the microthruster is mechanically clamped is suggested, but, contrary to what will be presented here, it does not seem to have been realized.

3. Experimentals

3.1. Design and materials

Ceramic microthrusters comprising five integrated parts: a platinum heater, a resistive platinum temperature sensor close to the heater, a catalytic bed, a catalytic chamber with a micronozzle, and a second temperature sensor placed above the catalytic chamber, Figure 1, were manufactured.

The design is based on the final design (called S/B/S) in [13], which exhibited the highest temperature tolerance, and has a heater and catalytic bed of 3.2 × 1.8 mm^2 and 3.2 × 4.3 mm^2, respectively.

3.2. Fabrication

The thrusters were built by stacking and laminating four layers of 150 μm thick alumina green tapes (ESL 44007-G/150, ElectroScience Laboratories, USA) that had been milled individually, and screen printed with platinum paste (ESL 5571-G). To make the catalytic bed porous, the plat-

inum paste was mixed with a sacrificial paste (ESL 4441) by 15%−20% of the volume. A graphite sacrificial insert that forms volatile products during sintering (ESL 49000), was placed in the catalytic chamber as a support during subsequent steps. A detailed manufacturing description is given in [13].

Before sintering, the contacts pads at the bottom side were connected to pads on the top by manually depositing platinum paste over the edge.

As silver is not compatible with sintering, it had to be added subsequently, notably to the interior of the sealed chamber. Therefore, it was in-situ electroplated on top of the porous Pt catalyst layer. An insulated wire was attached to the connection pad of the catalytic bed using conductive epoxy (CW2400, Chemtronics, USA). The sample was mounted with an o-ring to a tailor-made PCB clamp, connected to a syringe pump (PHD 2000, Harvard Apparatus, USA) via a tube and a NanoPort (PEEK 1532 and N-333, respectively, IDEX Health & Science, USA). This allowed for a steady flow of 0.8 ml/min of fresh plating solution through the device. The bed was electrochemically cleaned at 5 V for 5 min (ActiClean, Spa Plating, UK) and then plated for 20 min (Silver tank plating solution, Spa Plating, UK). Given the current density (5 mA/cm^2) and duration, the targeted thickness was 5 μm.

Three microthrusters were manufactured and characterized, one with Pt catalytic bed, one with Ag electroplated catalytic bed, and, finally, one reference sample without catalyst. For microscopy, separate metallization samples of the catalysts and non-porous platinum were prepared in addition. Furthermore, two thruster chips without lids (i.e., the top layer in Figure 1), one with a Pt and one with an Ag bed, were manufactured for cyclic voltammetry.

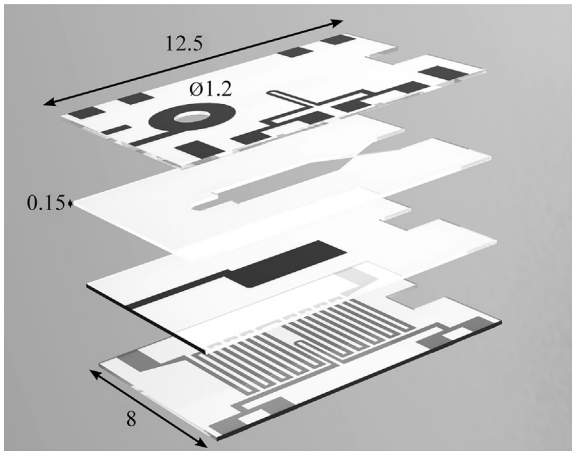

Figure 1 Exploded view of thruster design. Bottom up: floor layer with heater and temperature sensor, catalytic layer, chamber wall layer with nozzle, and lid layer with propellant inlet, connection pads and temperature sensor (loop in the centre), on top. Note that the bottom layer is flipped over here. The heater is actually facing down. All dimensions are in mm and before sintering, where the component shrinks by approximately 20%.

3.3. Characterization

The alignment and integrity of the sintered components were inspected using X-ray (XTV 130, Nikon, Japan), and the conductance of the electrical connections was measured using a multimeter (Fluke, 115 True RMS, USA).

The metallization samples were studied using atomic force microscopy (PSIA XE150 SPM/AFM, Park Systems, South Korea) and scanning electron microscopy, SEM, (Leo 440, Zeiss, Germany). The Gwyddion 2.47 software [35] was used to calculate the surface areas from the AFM images.

Cyclic voltammetry was performed on the Pt and Ag thruster chips without lids. One at a time, these were used as the working electrode in a three-electrode set-up controlled by a potentiostat (μAutolabIII, Metrohm, The Netherlands) with 50wt.% H_2O_2 as the electrolyte. The voltage was swept between −0.1 and 0.1 V with respect to an Ag/AgCl reference electrode, revealing higher catalytic activity as a higher current.

Probes (GKS 113 305 080 A 1502 C4A, Ingun, Germany) were used to make electrical contact to the thruster chips, which were held in place by screwing the inlet connection, a flangeless ferrule and nut (M-650 and M-660, IDEX Health & Science, USA), to an overhead stainless steel cantilever, Figure 2. To avoid electrical short-circuiting, a piece of alumina was firmly glued to the bottom side of the device with a ceramic adhesive (Ceramabond 569, Aremco, USA). To avoid point loads from the probes, spring washers were placed under the thrusters. Figure 2 shows a thruster chip mounted this way in the fixture, but, this far, only interfaced by the propellant inlet and two of the probes.

The quantitative comparison was based on the fact that a more effective catalyst produces more heat and therefore requires less external power to maintain a constant temperature of the device.

Ideally, all hydrogen peroxide should be decomposed and all water should be evaporated, wherefore only invisible vapor should exit the nozzle. Hence, observations of smoke and liquid at the nozzle output were qualitatively interpreted as non-ideal operation.

As the temperatures of the two integrated sensors have shown to be more or less equal below 300 °C [13], just the bottom one was used here. Before the firing test, this sensor was calibrated in a furnace, using a K-element thermocouple reference.

The propellant inlet was connected to a 5-ml glass microsyringe (VWR International, USA) with a H_2O_2 solution (50wt.%, Sigma-Aldrich, USA) put in a syringe pump (PHD 2000, Harvard Apparatus, USA), using 1/16″ PEEK tubing (IDEX Health & Science, USA).

MATLAB was used to control the power supply (QL355P, TTi, UK) connected to the heater, and a multimeter (34401A, Agilent, USA) that monitored the temperature sensor. While logging the temperature and the

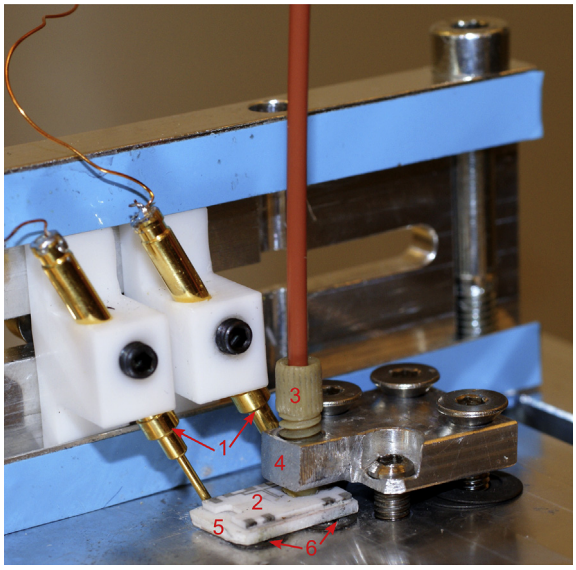

Figure 2 Close-up of a chip partly mounted in the stainless steel fixture to show two (out of six) probes (1), the chip (2), the inlet connection (3), the steel cantilever beam clamp (4), the alumina piece below the chip (5), and the spring washers (6).

consumed power (from the measured current and voltage of the power supply), the nozzle exit was monitored using a stereomicroscope.

The voltage of the heater power supply was ramped with 1.63 V/min, until 115 °C (just above the boiling point of 50wt.% H_2O_2) was reached. At this temperature, the pump was started with a flow of 15 µl/min. Next, the power required to maintain 115 °C at this flow, was measured. Correspondingly, the power required to maintain eight more temperatures, from 125 to 300 °C in steps of 25 °C, and five flow rates from 15 to 55 µl/min in steps of 10 µl/min, was measured. The upper temperature limit was decided based on the results of an initial study, measuring the maximum tolerable temperature of the inlet ferrule. Simultaneously, the temperature of the fixture was monitored using a thermocouple.

4. Results

Figure 3 shows the top and bottom side of a completed microthruster, as well as an X-ray image (right), where the alignment achieved between the different layers can be seen.

Both the non-porous and porous platinum surfaces have a larger effective surface area than the silver electroplated one, Figure 4. This is confirmed by the measured R_a (arithmetic averages of the surface topography) values, being 198, 396 and 33 nm for Pt, porous Pt, and Ag electroplated on the porous Pt surfaces, respectively. With Gwyddion, the actual surface areas of these scans were determined to 8.70×10^{-9}, 10.5×10^{-9}, and 8.12×10^{-9} mm^2, respectively. SEM images of the samples are shown in Figure 5.

For a given voltage, and averaging three sweeps from each sample, the nominal current density from the cyclic voltammetry was just a few percent higher for the Ag catalytic bed than for the Pt one. Taking into account the smoothening from electroplating, and dividing by the actual surface area, Ag exhibits close to 35% higher current density than Pt. However, although both catalysts yielded nice, linear current vs. voltage graphs, the Ag ones contained small steps, seemingly corresponding to bubbles forming despite the agitation.

As the flow and temperature, as well as the catalyst, were varied, the exhaust varied. Three main regimes were observed: liquid, clearly visible smoke, and invisible vapor, as detected by condensate on a glass slide. In addition, some conditions resulted in spitting. When this occurred, the sound from the rocket changed from hissing to a distinct pattering. Table 1 categorises the various exhaust types observed.

Below 200 °C, the reference thruster, lacking catalyst, ran steadily only at the lowest flow, Table 2. At 200 °C and above, spitting in combination with smoke occurred above 15 µl/min. At 225 °C, when the flow was increased to 45 µl/min, the component cracked after 1 min. Flooding was observed only for this type of thruster.

Both for the Ag and the Pt catalysts, a flow of 15 µl/min resulted in smoke at all temperatures below 225 °C, Tables 3 and 4. The Pt one sometimes displayed a pulsing behavior, switching between exhausting pure smoke and a combination of vapor and droplets (see the complimentary videos), for a few seconds each. At temperatures from 115 to 200 °C, small amounts of liquid were visible in the exhaust of the Ag thruster for flows of 45 and 55 µl/min. The Ag thruster started spitting at 15 µl/min when the temperature was 200 °C, whereas the Pt thruster displayed stable smoke under the same condition, but pulsed at increased flow. At

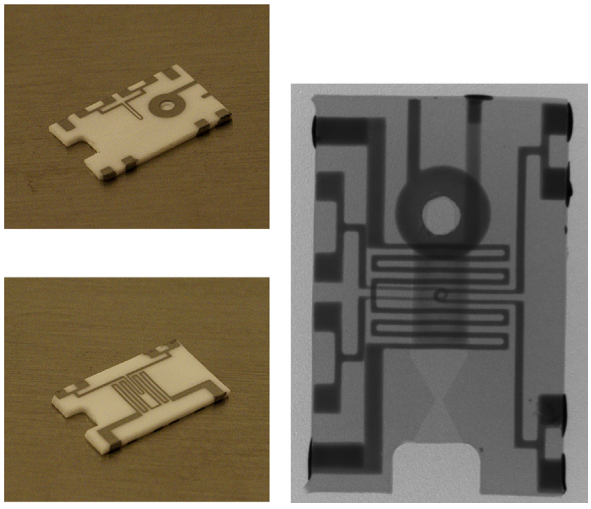

Figure 3 Top and bottom of a completed microthruster (left), and an X-ray image (right) revealing the catalytic bed. The loops meeting at the centre of the heater are the temperature sensors on the top and bottom of the chip. The electrical connections over the edges are the darkest parts of the device, whereas the lightest part is the cavity with the inlet and nozzle.

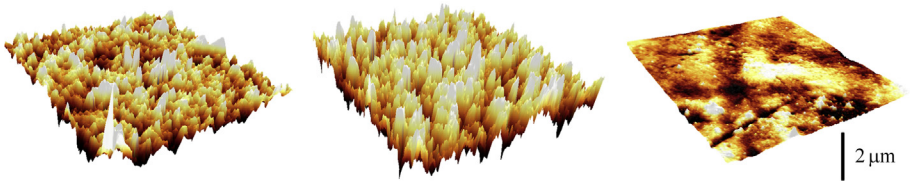

Figure 4 AFM surface topography of platinum (left), porous platinum (middle) and silver electroplated porous platinum (right) surfaces. Scanned areas are 90 × 90 µm^2. The vertical magnification differs from the lateral one.

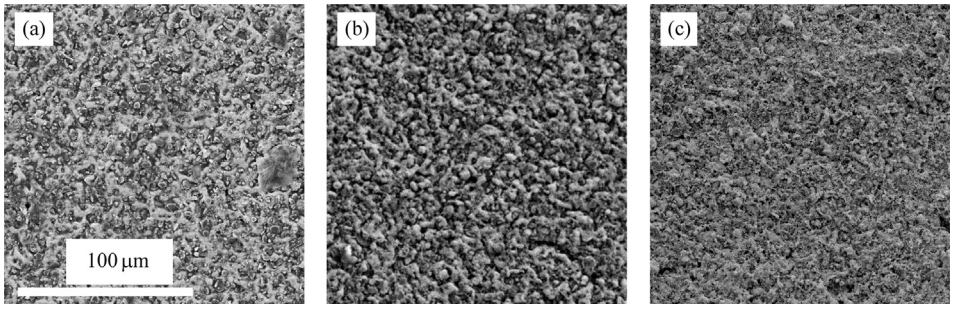

Figure 5 SEM images of platinum (a), porous platinum (b), and silver electroplated on porous platinum (c) surfaces.

250 °C and above, the Pt thruster did not expel smoke anymore, whereas the Ag one did at 250 °C. Regions with spitting were found for all thrusters, and there was no distinct border between where only smoke/vapor is present, and where also spitting occurs.

Whereas the Pt thruster survived all temperatures, the Ag one cracked after the 250 °C measurement, on raising the temperature to 275 °C.

For each temperature and flow rate setting, the average power needed to maintain the temperature of the samples was calculated from the current measured through, and the voltage applied to, the heater of the samples. The power required to heat the dry thrusters without catalyst, and with Ag and Pt catalyst to 115 °C, was 4.9, 5.5, and 4.8 W, respectively, indicates that the boundary conditions differed. With few exceptions, it was still observed that the power consumption increased with increasing temperature and

Table 1 Various exhaust types observed during wet running of the microthrusters, and their colour assignment for later use.

Exhaust type	Color assignment
Smoke	
Smoke and some visible liquid in the outlet	
Vapor	
Pulsing between smoke and vapor	
Flooding	
Region of spitting	

Table 2 Qualitative observations during firing of the reference microthruster, lacking catalyst. Cracking is indicated with X.

Flow rate /(µl/min)	Temperature/°C								
	115	125	150	175	200	225	250	275	300
15							---	---	---
25		---	---	---			---	---	---
35		---	---	---			---	---	---
45	---	---	---	---	---	X	---	---	---
55	---	---	---		---	---	---	---	---

Table 3 Qualitative observations during firing of a microthruster with Ag as catalyst. Cracking is indicated with X.

Flow rate /(µl/min)	Temperature/°C								
	115	125	150	175	200	225	250	275	300
15								X	---
25								---	---
35								---	---
45						---	---	---	---
55						---	---	---	---

Table 4 Qualitative observations during firing of a microthruster with Pt as catalyst.

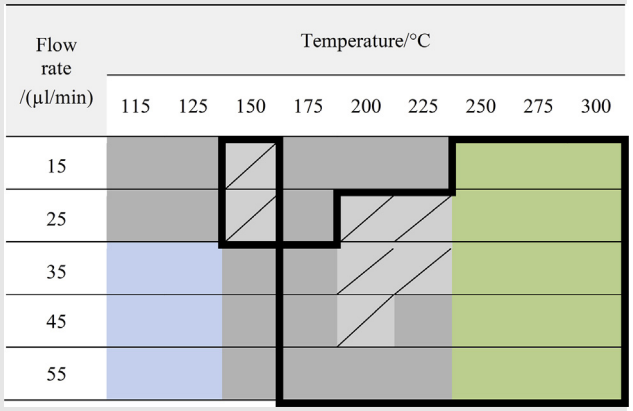

increasing flow rate. For the Ag and Pt samples, the increase was more obvious at higher flow rates. For the Pt sample, at temperatures above 200 °C, there was no outlier from the general trend. In fact, the increase of power with increase of flow rate became clearer. Even if the sample-specific power needed to reach 115 °C for zero flow is subtracted, there is, however, no clear difference between the two catalysts.

The fact that the temperature of the fixture was nearly 40 °C, indicates that a substantial part of the power was lost to it. Despite this, the fixture was a great improvement to the setup in [15].

5. Discussion

The small amounts of liquid sometimes seen in the exhaust of the Ag thruster, but not for the Pt thruster, and this thruster's spitting, clearly indicate that Pt is a more efficient catalyst. Also, at 250 °C and above, the Pt thruster didn't expel smoke anymore, whereas the Ag thruster did.

The higher actual current density of Ag obtained during voltammetry is interpreted as Ag being an inherently more efficient catalyst. However, under the conditions here, and according to the results of the firing test, where the catalytic bed is accessed differently and probably less uniformly, there is no efficiency gained from using a silver layer. Also, the risk of catalyst degradation of silver is in favor of platinum.

The power lost to the probes, and the thermal convection and radiation can be assumed similar for all the chips, but the heat dissipation to the fixture base plate varies. This made comparison between the powers needed to sustain a certain temperature for the different catalysts somewhat difficult. The fact that the thrusters operated in different regimes at different temperatures, where the elements of spitting is particularly hard to quantify, adds to the difficulty. To compensate for the different boundary conditions, the zero-flow power needed to reach 115 °C was subtracted from all powers used in the firing experiments.

Table 5 Heat capacities and heat of vaporization and decomposition as well as density for 50wt.% H_2O_2.

	H_2O_2, 50wt.%	H_2O	O_2
Heat capacity of liquid /(J/(g·°C)) [36]	3.31	4.20	
Heat capacity of gas at 150 °C, atmospheric pressure /(J/(g·°C)) [37]	–	1.91	0.95
Heat of vaporization/(kJ/g) [36]	2.00	2.44	
Heat of decomposition/(kJ/g) [36]	1.40		
Boiling point/°C [38]	114		
Density/(g/ml) (ρ) [38]	1.19		

For optimal firing, energy is needed to heat the 50wt.% hydrogen peroxide first to boiling, then to vaporization, and finally, to heat the vapors. When hydrogen peroxide decomposes, there is an energy gain caused by the heat of decomposition, and the resulting gases, i.e., oxygen and water vapor, can be heated further. By comparing the heat of vaporization and the heat of decomposition (see references below), one finds that concentrations above about 64% allow for a self-sustained decomposition. Table 5 presents data that can be used to approximate the power needed for heating and evaporating hydrogen peroxide at different flows.

With data from Table 5, the energy, Q, needed to heat a liquid or gas with a heat capacity of $C_{p,l}$, can be calculated from $Q = C_{p,l} \times m \times \Delta T$, where m is the mass, and ΔT is the temperature increase. The energy cost of vaporization and the energy gained from decomposition are calculated from the heat values in the same table. (Here, the heat capacity of hydrogen peroxide vapor, is approximated with that of water vapor.) To translate Q to power consumption, P, the mass flow rate, calculated from the volume flow rate and density, is used. Since the power losses to the surrounding are unknown, it is not possible to directly compare the theoretical power consumptions with the measured ones. However, it is possible to compare the experimentally obtained power needed to go from a flow rate to the next higher one with the power increase calculated.

An extreme is where pure liquid at a temperature of 114 °C exits the nozzle, corresponding to a power increase of 0.06 W over the whole temperature range when the flow increases by 10 μl/min. Another extreme represents complete decomposition, with the resulting vapor having the same temperature as the component. The power increase needed for this depends on temperature, but is approximately 0.2 W for a flow increase of 10 μl/min. A third extreme is when hydrogen peroxide is evaporated without first being decomposed. For this, approximately 0.5 W is needed. The energy consumptions for the observed cases are expected to be in-between these extremes, Figure 6.

The majority of the data points in Figure 6 are located between the extreme boundary planes. Especially for mid-range temperatures, it is notable that the power increase

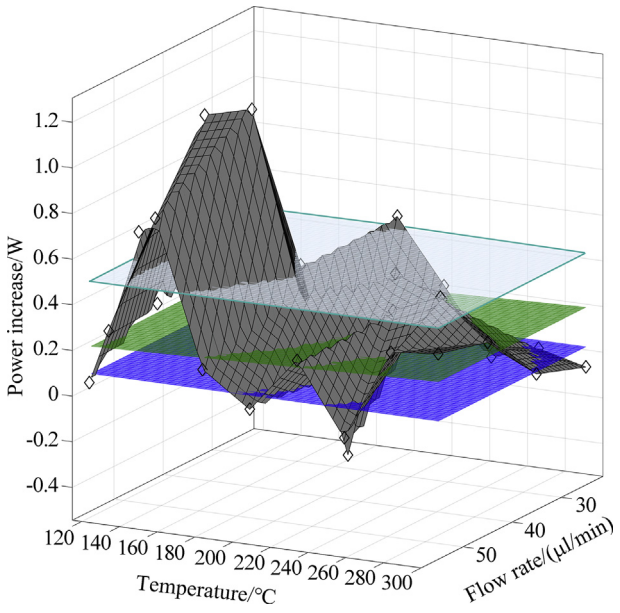

Figure 6 Calculated (semi-transparent planes), and experimentally obtained powers needed to increase the flow by 10 µl/min at different temperatures for the Pt thruster (data points). The surface fitting of the data points is just for guidance. The calculations were done for three reference scenarios: heating H_2O_2 to 114 °C without evaporation and decomposition (bottom plane), heating H_2O_2 to its boiling point, evaporating it, and heating the vapor without decomposition (top plane) and finally, allowing for full decomposition of hydrogen peroxide with water vapor and oxygen gas heated to the thruster temperature as the only result (middle plane).

needed with increasing flow, varies a lot. Whereas operation at high temperature demands less power increase, and, occasionally, even a decrease, as expected from catalytic combustion, the generation of smoke and the mere pulsing between regimes at lower temperatures, require more power. To some degree, one can correlate the three main domains of exhaust types in the table (columns 1−2, 3−6, and 7−9) with the ridges and valleys of the surface of data points in Figure 6. From this, one can see that transiting between smoke and smoke and vapor pulsing operation is of less concern than transiting between pure smoke operation to the higher flow rates, where liquid is gathering in the outlet. However, it is not clear why this should require less power.

The high chemical resistance of alumina makes it a promising material for many liquid propellants. However, alumina has a rather low resistance to thermal shock [39]. Feeding a hot thruster with a liquid results in large temperature gradients and transients that may result in thermal shock and fracturing. To mitigate this, the propellant can be evaporated before entering the ceramic thruster, or an injector can be used to atomize the liquid.

After this exploratory, yet crucial, investigation of catalyst materials behavior, the next step would be measuring the thruster's performance in terms of thrust and specific impulse using space-grade hydrogen peroxide.

6. Conclusion

A new method to increase the porosity, and hence the surface area, of a platinum catalytic bed, using a carbon-platinum paste, has been successfully demonstrated. In addition, post-sintering, inter-cavity plating has been shown a viable way of circumventing the limitations with metallization in HTCC technology. Hot firing of thrusters with and without metallization inside the fluidic chamber, clearly shows that operation without a catalyst is not viable, and also confirms the catalytic effect of both platinum and silver for 50wt.% H_2O_2. In terms of power consumption, and contrary to literature, the difference between the two catalysts was found to be small. Contrary to the separate voltammetry, Pt was found to perform slightly better than Ag in reality. Also, it is concluded that the Pt catalyst thruster is far more stable than the Ag one.

Acknowledgements

The Swedish National Space Board and the Centre for Natural Disasters Science (CNDS) are acknowledged for project funding. The Knut and Alice Wallenberg Foundation is acknowledged for funding the laboratory facilities. Peter Sturesson at the Department of Engineering Sciences, Uppsala University is gratefully thanked for help with the SEM. Dhananjay V. Barbade, who participated in the previous study, is appreciated for inspiration to this work.

Appendix A. Supplementary data

Complementary videos to this article can be found online at https://doi.org/10.1016/j.jppr.2020.08.003.

References

[1] W.J. Larson, J.R. Wertz, Space Mission Analysis and Design, third ed., Kluwer American Publishers, 1999.
[2] J. Mueller, C. Marrese, J. Polk, E.H. Yang, A. Green, V. White, D. Bame, I. Chadraborty, S. Vargo, An overview of MEMS-based micropropulsion developments at JPL, J. Acta Astronaut. 52 (9/12) (2003) 881−895.
[3] C. Rossi, Micropropulsion for space - a survey of MEMS-based micro thrusters and their solid propellant technology, J. Sensors Updat. 10 (1) (2002) 257−292.
[4] E.J. Wernimont, System trade parameter comparison of monopropellants: hydrogen peroxide vs hydrazine and others, in: Proc. 42nd AIAA/ASME/SAE/ASEE Joint Propulsion Conference & Exhibit, 2006.
[5] M. Ventura, E. Wernimont, S. Heister, S. Yuan, Rocket grade hydrogen peroxide (RGHP) for use in propulsion and power devices - historical discussion of hazards, in: Proc. 43rd AIAA/ASME/-SAE/ASEE Joint Propulsion Conference & Exhibit, 2007.
[6] ECHA, Support Document Member State Committee, Support Document for Identification of Hydrazine as a Substance of Very High Concern Because of its CMR Properties, 2011.
[7] P. Pędziwiatr, F. Mikoøajczyk, D. Zawadzki, K. Mikoøajczyk, A. Bêdka, Decomposition of hydrogen peroxide-kinetics and review of chosen catalysts, Acta Innov. (26) (2018) 45−52.

[8] C.G. Freyschlag, R.J. Madix, Precious metal magic: catalytic wizardry, Mater. Today 14 (4) (2011) 134−142.
[9] K.D. Patel, M.S. Bartsch, M.H. McCrink, J.S. Olsen, B.P. Mosier, R.W. Crocker, Electrokinetic pumping of liquid propellants for small satellite microthruster applications, J. Sensors Actuators B Chem. 132 (2) (2008) 461−470.
[10] L.C. Liu, A. Corma, Metal catalysts for heterogeneous catalysis: from single atoms to nanoclusters and nanoparticles, Chem. Rev. 118 (10) (2018) 4981−5079.
[11] D. Krejci, A. Woschnak, C. Scharlemann, K. Ponweiser, Hydrogen peroxide decomposition for micro propulsion: simulation and experimental verification, in: Proc. 47th AIAA/ASME/SAE/ASEE Joint Propulsion Conference & Exhibit, 2011.
[12] V. Domnich, Y. Aratyn, W.M. Kriven, Y. Gogotsi, Temperature dependence of silicon hardness: experimental evidence of phase transformations, Rev. Adv. Mater. Sci. 17 (2008) 33−41.
[13] Z. Khaji, L. Klintberg, D. Barbade, K. Palmer, G. Thornell, Endurance and failure of an alumina-based monopropellant microthruster with integrated heater, catalytic bed and temperature sensors, J. Micromech. Microeng. 27 (5) (2017) 055011.
[14] M. Ventura, E. Wernimont, Advancements in high concentration hydrogen peroxide catalyst beds, in: Proc. 37th AIAA Jt. Propuls. Conf. Exhib., 2001.
[15] C. Bramanti, A. Cervone, L. Romeo, L. Torre, L. D'Agostino, A.J. Musker, G. Saccoccia, Experimental characterization of advanced materials for the catalytic decomposition of hydrogen peroxide, in: Proc. 42nd AIAA/ASME/SAE/ASEE Joint Propulsion Conference & Exhibit, 2006.
[16] L. Pirault-Roy, R. Eloirdi, M. Guérin, C. Kappenstein, N. Pillet, Hydrogen peroxide decomposition on various supported catalysts effect of stabilizers, J. Propul. Power 18 (6) (2002) 1235−1241.
[17] J.J. Rusek, New decomposition catalysts and characterization techniques for rocket-grade hydrogen peroxide, J. Propul. Power 12 (3) (1996) 574−579.
[18] A. Cervone, L. Romeo, L. Torre, L. D'Agostino, F. Calderazzo, A.J. Musker, G.T. Roberts, G. Saccoccia, Development of green hydrogen peroxide monopropellant rocket engines and testing of advanced catalytic beds, in: Eur. Sp. Agency, Spec. Publ. ESA SP, no. SP-635, 2006.
[19] A. Cervone, L. Romeo, L. Torre, L. D'Agostino, F. Calderazzo, A.J. Musker, G.T. Roberts, G. Saccoccia, Development of green hydrogen peroxide monopropellant rocket engines and testing of advanced catalytic beds, in: Proc. 3rd International Conference on Green Propellants, 2006.
[20] R. Eloirdi, S. Rossignol, C. Kappenstein, D. Duprez, Catalytic decomposition of different monopropellants, in: Proc. 3rd International Conference on Spacecraft Propulsion, 2000, pp. 263−270.
[21] K. Takahashi, T. Ikuta, Y. Dan, K. Nagayama, M. Kishida, Catalytic porous microchannel for hydrogen peroxide MEMS thruster, in: Proc. The 23rd Sensor Symposium, 2006, pp. 513−516.
[22] D.L. Hitt, C.M. Zakrzwski, M.A. Thomas, MEMS-based satellite micropropulsion via catalyzed hydrogen peroxide decomposition, J. Smart Mater. Struct. 10 (6) (2001) 1163−1175.
[23] P. Kundu, A.K. Sinha, T.K. Bhattacharyya, S. Das, MnO_2 nanowire embedded hydrogen peroxide monopropellant MEMS thruster, J. Microelectromech. Syst. 22 (2) (2013) 406−417.
[24] V. Lekholm, A. Persson, K. Palmer, F. Ericson, G. Thornell, High-temperature zirconia microthruster with an integrated flow sensor, J. Micromech. Microeng. 23 (5) (2013) 55004.
[25] K.H. Cheah, K.S. Low, Fabrication and performance evaluation of a high temperature co-fired ceramic vaporizing liquid microthruster, J. Micromech. Microeng. 25 (1) (2014) 15013.
[26] K. Karthikeyan, S.K. Chou, L.E. Khoong, Y.M. Tan, C.W. Lu, W.M. Yang, Low temperature co-fired ceramic vaporizing liquid microthruster for microspacecraft applications, J. Appl. Energy 97 (2012) 577−583.
[27] K.L. Zhang, S.K. Chou, S.S. Ang, Development of a low-temperature co-fired ceramic solid propellant microthruster, J. Micromech. Microeng. 15 (5) (2005) 944−952.
[28] J. Thakur, R. Pratap, Y. Fournier, T. Maeder, P. Ryser, Realization of a solid-propellant based microthruster using low temperature co-fired ceramics, Sensors Transducers 117 (6) (2010) 29−40.
[29] M.H. Wu, R.A. Yetter, A novel electrolytic ignition monopropellant microthruster based on low temperature co-fired ceramic tape technology, Lab Chip 9 (7) (2009) 910−916.
[30] K. Markandan, Z. Zhang, J. Chin, K.H. Cheah, H.B. Tang, Fabrication and preliminary testing of hydroxylammonium nitrate (HAN)-based ceramic microthruster for potential application of nanosatellites in constellation formation flying, Microsyst. Technol. 25 (2019) 4209−4217.
[31] D. Plumlee, J. Steciak, A. Moll, Development and simulation of an embedded hydrogen peroxide catalyst chamber in low-temperature co-fired ceramics, Int. J. Appl. Ceram. Technol. 4 (5) (2007) 406−414.
[32] K.H. Cheah, P.S. Khiew, J.K. Chin, Fabrication of a zirconia MEMS-based microthruster by gel casting on PDMS soft molds, J. Micromech. Microeng. 22 (9) (2012) 095013.
[33] P. Kundu, T. Bhattacharyya Kanti, S. Das, Design, fabrication and performance evaluation of a vaporizing liquid microthruster, J. Micromech. Microeng. 22 (2) (2012) 025016.
[34] W. Sun, G. Cai, N. Donadio, B. Kuo, J. Lee, R.A. Yetter, Development of meso-scale co-fired ceramic tape axisymmetric combustors, Int. J. Appl. Ceram. Technol. 9 (4) (2012) 833−846.
[35] D. Nečas, P. Klapetek, Gwyddion: an open-source software for SPM data analysis, Open Phys. 10 (1) (2012) 181−188.
[36] P.A. Giguère, B.G. Morissette, A.W. Olmos, O. Knop, Hydrogen peroxide and its analogues: VII. Calorimetric properties of the systems H_2O-H_2O_2 and DO_2-D_2O_2, Can. J. Chem. 33 (5) (1955) 804−820.
[37] A.K. Coker, Ludwig's Applied Process Design for Chemical and Petrochemical Plants: Distillation, Packed Towers, Petroleum Fractionation, Gas Processing and Dehydration, fourth ed., Gulf Professional, 2010.
[38] W.C. Schumb, C.N. Satterfield, R.L. Wentworth, Hydrogen Peroxide, Reinhold Pub. Corp., New York, 1955.
[39] P. Auerkari, Mechanical and Physical Properties of Engineering Alumina Ceramics, Technical Research Centre of Finland, Espoo, Finland, 1996.